Published in final edited form as:
Mol Immunol. 2013 December 31; 56(4): 768–780. doi:10.1016/j.molimm.2013.07.001.

The Zinc Finger Transcription Factor ZXDC Activates CCL2 Gene Expression by Opposing BCL6-mediated Repression

Jon E. Ramsey and **Joseph D. Fontes***
Department of Biochemistry and Molecular Biology, 3901 Rainbow Blvd. MS3030, University of Kansas School of Medicine, Kansas City, Kansas, 66160 U.S.A

Jon E. Ramsey: jramsey@kumc.edu; Joseph D. Fontes: jfontes@kumc.edu

Abstract

The zinc finger X-linked duplicated (ZXD) family of transcription factors has been implicated in regulating transcription of major histocompatibility complex class II genes in antigen presenting cells; roles beyond this function are not yet known. The expression of one gene in this family, ZXD family zinc finger C (ZXDC), is enriched in myeloid lineages and therefore we hypothesized that ZXDC may regulate myeloid-specific gene expression. Here we demonstrate that ZXDC regulates genes involved in myeloid cell differentiation and inflammation. Overexpression of the larger isoform of ZXDC, ZXDC1, activates expression of monocyte-specific markers of differentiation and synergizes with phorbol 12-myristate 13-acetate (which causes differentiation) in the human leukemic monoblast cell line U937. To identify additional gene targets of ZXDC1, we performed gene expression profiling which revealed multiple inflammatory gene clusters regulated by ZXDC1. Using a combination of approaches we show that ZXDC1 activates transcription of a gene within one of the regulated clusters, chemokine (C-C motif) ligand 2 (CCL2; monocyte chemoattractant protein 1; MCP1) via a previously defined distal regulatory element. Further, ZXDC1-dependent up-regulation of the gene involves eviction of the transcriptional repressor B-cell CLL/lymphoma 6 (BCL6), a factor known to be important in resolving inflammatory responses, from this region of the promoter. Collectively, our data show that ZXDC1 is a regulator in the process of myeloid function and that ZXDC1 is responsible for *Ccl2* gene de-repression by BCL6.

Keywords

zinc finger transcription factor; gene regulation; inflammation; chemokine

1. Introduction

Innate immunity relies upon the timely and highly regulated expression of cytokines to alert and attract sentinel leukocytes to sites of pathogenic breaching, wound healing and inflammation. The recruitment of monocytes and granulocytes to areas of inflammation is mediated, in large part, by the activated expression of chemokines by cells residing at inflammatory foci. Furthermore, exposure of leukocytes to cytokines results in the induction

*Corresponding author, Phone: (913) 588-9848.

or repression of a large number of genes associated with inflammation (Le et al., 2004). Defective innate immune response regulation, whereby cytokine signaling is either unprovoked or prolonged, underlies inflammatory disease (Theofilopoulos et al., 2010).

Chemokine (C-C motif) ligand 2 [CCL2; also referred to as monocyte chemoattractant protein 1 (MCP-1)] plays a decisive role in recruiting monocytes to sites of inflammation (Rahimi et al., 1995; Rollins et al., 1991). Transcription of CCL2 is controlled by an array of *cis*-acting elements which are bound by transcription factors in both a cell type- and stimuli-specific manner. These regulatory elements are clustered within two control regions: a 200bp proximal regulatory region (PRR) near the transcriptional start site and the distal regulatory region (DRR), located approximately 2.6 kbp upstream of the transcriptional start site (Ping et al., 1996; Ueda et al., 1994). The PRR is indispensable for transcription and harbors binding sites for Sp1 and NF-κB that become occupied in response to tumor necrosis factor alpha (TNFα) stimulation (Boekhoudt et al., 2003; Martin et al., 1997; Ping et al., 1999; Ping et al., 1996; Ueda et al., 1994). In addition, an AP-1 site (tetradecanoylphorbol acetate responsive element; TRE) in the PRR mediates transcription activated by diverse stimuli (Martin et al., 1997; Shyy et al., 1995). Full activation of *Ccl2* transcription requires the DRR, which also contains NF-κB (Boekhoudt et al., 2003; Teferedegne et al., 2006) and AP-1 sites (Cho et al., 2002; Freter et al., 1995). NF-κB bound to the DRR recruits CBP/p300, which catalyzes histone acetylation across the DRR-PRR region and facilitates binding of Sp1 and NF-κB to the PRR (Boekhoudt et al., 2003). Direct communication between the PRR and DRR occurs through looping mediated by NF-κB, Sp1 and CBP/p300 and this event precedes association of co-activator associated arginine methyltransferase 1 (CARM1), a co-activator necessary for *Ccl2* activation (Covic et al., 2005; Teferedegne et al., 2006).

CCL2 transcription is also subject to repression by B-cell/CLL lymphoma 6 (BCL6), a BTB/POZ (Bric-brac, Tramtrack, Broad complex/Poxvirus zinc finger) family transcription factor that is critical for germinal center (GC) formation (Dent et al., 1997). Interestingly, $BCL6^{-/-}$ mice not only display defects in GC formation and high-affinity antibody production, but also demonstrate severe, widespread inflammation (Dent et al., 1997; Ye et al., 1997). These observations led to the finding that BCL6 regulates cytokine production in multiple cell types, particularly macrophages (Toney et al., 2000). In macrophages, BCL6 interacts with DNA elements that are often within nucleosomal distance of enhancers occupied by NF-κB (p65) during LPS activation. In a majority of cases, occupancy of BCL6 and p65 is mutually exclusive, suggesting that these factors form opposing cistromes (Barish et al., 2010). BCL6 and p65 antagonistically regulate a long list of genes including *Ccl2* as well as other genes within the *Ccl* locus on mouse chromosome 11. Repression by BCL6 is primarily via direct or indirect recruitment of multiple histone deacetylase (Barish et al., 2012; Dhordain et al., 1997; Huynh and Bardwell, 1998; Huynh et al., 2000; Lemercier et al., 2002)

We identified a transcription factor, ZXD family zinc finger C (ZXDC) that, along with its family member ZXDA, forms a complex with the class II trans-activator (CIITA), an interaction necessary for robust activation of MHC class II genes by CIITA (Al-Kandari et al., 2007b). Outside of the zinc finger region, the ZXD proteins show little homology with other transcription factors and besides their role in MHC class II transcription, nothing is known about their function.

In this study we demonstrate that *ZXDC* regulates transcription of key genes during myeloid cell differentiation and the inflammatory response elicited by AP-1 activation by phorbol 12-myristate 13-acetate (PMA). Knockdown and over-expression of the largest *ZXDC* isoform, ZXDC1, in U937 cells affected their macrophage-like differentiation in a manner that indicates *ZXDC* contributes to the differentiation program. Gene expression profiling

demonstrated that ZXDC1 manipulation affects genes associated with differentiation and inflammation, including the chemokine CCL2. We found that over-expression of ZXDC1 leads to increased CCL2 mRNA levels, an effect that requires the DRR of the CCL2 promoter. This increase in CCL2 mRNA results from ZXDC1 binding to and inhibiting BCL6 function; knockdown of ZXDC1 lead to greater occupancy of the CCL2 promoter by BCL6. Overall, our data support a model whereby ZXDC1 supports lineage-specific and inflammatory gene expression through a mechanism that, at least in part, involves alleviating BCL6-mediated transcriptional repression of inflammatory genes.

2. Materials and methods

2.1. Cell Culture and Reagents

Cell lines U937 [American Type Culture Collection (ATCC): CRL-1593.2] and Raji (ATCC: CCL-86) were maintained in RPMI 1640 (Mediatech, Inc., Manassas, VA) containing 10% FBS (Atlanta Biologicals, Inc., Lawrenceville, GA) and 100 U/mL penicillin and 100 ug/mL streptomycin (Life Technologies, Inc. Carlsbad, CA) at 37°C, 5% CO_2. HEK293 cells (ATCC: CRL-1573) and HEK293T (Thermo Fisher Scientific, Inc., Waltham, MA) were cultured in DMEM supplemented as above. Differentiating agent phorbol 12-myristate 13-acetate (PMA) (Sigma-Aldrich, Inc., St. Louis, MO) and prepared as a 1000× solution in dimethylsulfoxide (DMSO). For differentiation of U937, cells were plated at densities of 1×10^5 cells/mL for treatment with vehicle (Veh, 0.1% DMSO), 4×10^5 cells/mL for treatment with PMA (100 nM). Cells were allowed to differentiate for various times as indicated in figure legends.

2.2. Plasmids

The ZXDC1, ZXDC2 and BCL6 open reading frames were subcloned into the lentiviral expression plasmid pCDH-MSCV-MCS-EF1-GFP-Puro (referred to herein as pCDH; System Biosciences, Inc., Mountain View, CA). The source clones were as follows: ZXDC1, pCMV-Sport6-ZXDC1 (GenBank accession no. AL553476; Life Technologies, Inc.); BCL6, pCMV-Sport6-BCL6 (IMAGE clone 40148809; Thermo Fisher Scientific, Inc.); ZXDC2, pCMV-Sport6-ZXDC2 was generated by subcloning the BglII-NotI fragment of pCMV ZXDC2.2 [IMAGE clone ID 39655, (Aleksandrova et al., 2009)] into pCMV-Sport6-ZXDC1. N-terminal FLAG-tagged ZXDC1 was constructed in plasmid pCDNA3 into which the coding sequence for an N-terminal 3×FLAG epitope had been inserted. Hemaglutinin (HA)-tagged BCL6 constructs were a kind gift of R. Dalla-Favera (Bereshchenko et al., 2002; Chang et al., 1996). A doxycycline inducible microRNA-adapted shRNA (shRNAmir) construct specific for ZXDC (pTRIPZ clone ID: V3THS-381738), in addition to a non-silencing control construct (pGIPZ plasmid backbone) was purchased from a commercial supplier (Expression Arrest™ TRIPZ lentiviral shRNAmir; Thermo Fisher Scientific, Inc.). The non-silencing control shRNAmir was sub-cloned into pTRIPZ according to the manufacturer's instructions. Short-hairpin RNA (shRNA) directed against human ZXDC1 (NCBI accession: NM_025112) were cloned into plasmid pGreenPuro (System Biosciences, Inc.) according to the manufacturer's instructions. A shRNA directed against firefly luciferase was supplied by the manufacturer and used as a negative control. Sequences of shRNA can be found in Supplemental Table 1. Reporter plasmids were generated by PCR-mediated subcloning of genomic *Ccl2* sequence, limited by the given coordinates, into the *MluI- KpnI* sites of pCMV-Gluc (New England Biolabs, Inc.). Deletion constructs were made by restriction digest and re-ligation at the given coordinates.

2.3. Whole Cell Extraction

For preparation of protein lysates, U937 cells were harvested, washed once in ice-cold phosphate buffered saline and resuspended in Lysis Buffer [25 mM Tris-HCl pH 7.5, 0.5% SDS, 0.5 mM EDTA, 1X Halt Protease Inhibitor Cocktail (Thermo Fisher Scientific, Inc.) and 50 Units/mL Benzonase (Novagen/EM4D Biosciences, San Diego, CA)]. Lysates were incubated on ice for 10 minutes and centrifuged at 20,000g, 4°C, 10 minutes to remove insoluble material. Lysates were assayed for total protein concentration using the Bio-Rad Protein Assay Reagent (Bio-Rad Laboratories, Inc., Hercules, CA) according to manufacturer's instruction, with bovine serum albumin (Sigma-Aldrich, Inc.) dissolved in Lysis Buffer as a standard.

2.4. Lentivirus Production and Transduction

Lentiviral particle packaging was performed as described (Marino et al., 2003), with the following modifications. HEK293T cells were seeded at a density of 6.5×10^6 cells per 15 cm dish in DMEM media 24 hours prior to transfection. For packaging of 2nd generation lentiviral particles, 25 μg of expression plasmid (either pGreenPuro:shRNA or pCDH, 10 μg envelope plasmid pMD2.g (Addgene plasmid 12259, deposited by D. Trono) and 15 μg packaging plasmid psPAX2 (Addgene plasmid 12260, deposited by D. Trono) (Naldini et al., 1996) were transfected via calcium phosphate precipitation. Packaging of third generation vectors was performed essentially as described above, however, 20 μg pTRIPZ:shRNAmir, 10 μg pMD2.g and 10 μg each packaging plasmids pMDLg/pRRE and pRSV-Rev [Addgene plasmids 12251 and 12253, respectively (Dull et al., 1998)] were used. Media was replaced 4 hours post-transfection. Approximately 16 hours post-transfection, caffeine was added to the media to a final concentration of 4 mM (Ellis et al., 2011). Lentiviral particles were harvested 48 hours post-transfection, filtered and centrifuged at 30,000g, 15°C, for two hours. Pelleted lentiviral particles were resuspended in RPMI 1640 and stored at −80°C. Titers of pCDH- and pGreenPuro-derived vectors were determined by transducing 50,000 U937 in 0.5 mL growth media in 24 well plates with various dilutions of lentiviral supernatant and measuring the percentage of GFP positive cells by flow cytometry (Becton-Dickinson LSRII) 48 hours post transduction.

Transduction of U937 for stable ZXDC1/2 overexpression or knockdown was performed by adding concentrated lentivirus to 1×10^6 cells at a multiplicity of infection (MOI) of 10 and allowing infection to proceed 24 hours under normal incubation conditions. Cells were washed with growth media and re-plated at a density of 1.5×10^5 cells/mL to expand for 3 days. Stable transduction with pTRIPZ-derived lentiviral constructs were performed essentially the same way. After 3 days of recuperation, positively transduced cells were selected by treatment with 1 μg/mL puromycin (InvivoGen, Inc., San Diego, CA), until viability returned to >90% (approximately 1–2 weeks). Stable polyclonal cell lines were maintained in 0.5 mg/mL puromycin. For inducible knockdown, cells were plated at a density of 1×10^5 cell/mL in standard growth media and treated with 0.5 μg/mL freshly prepared doxycycline in Dulbecco's PBS (doxycycline hyclate; MP Biomedical, LLC). Doxycycline was supplemented again after 24 hours. After 48 hours of doxycycline treatment, cells were re-plated at a density of 1×10^5 cell/mL for vehicle treatment, or 4×10^5 cell/mL for PMA treatment (100 nM) and allowed to differentiate for 72 h. Doxycycline was supplemented at the time of vehicle or PMA treatment and again 24 hours later.

2.5. Generation of stable Ccl2 promoter reporter cell lines

U937 were electroporated with 5 μg of pCcl2-GLuc reporter plasmids, linearized with *PstI* (New England Biolabs) using InGenio Electroporation solution (Mirus Bio, LLC, Madison, WI) according to the manufacturer's recommendations. Briefly, 2.5×10^6 cells were resuspended in 250 μL of solution, placed in a 4 mm electroporation cuvette (BioSmith,

Inc., San Diego, CA) to which the linearized plasmid, in a volume of 12.5 μL, was added. The cells were electroporated in a Bio-Rad GenePulser Xcell (Bio-Rad Laboratories, Inc.) by applying a single pulse (exponential decay, 960 μF, 250 V). Cells were immediately removed from the cuvette and placed in 3 mL of growth media and allowed to recover for 48 hours prior to re-plating and selection with 0.8 mg/mL G418. Once highly viable, stable, polyclonal cell lines were established, cultures were maintained in 0.4 mg/mL G418.

2.6. Stable cell line reporter assays

Stable reporter cell lines were transduced with lentivirus at a MOI of 10 in triplicate and allowed to expand for 72 hours. As indicated in the results, mixtures of various lentiviral particles were sometimes used. Gaussia luciferase expression was measured with the BioLux *Gaussia* Luciferase Assay Kit (New England Biolabs, Inc.) using a $20/20^{n}$ luminometer (Turner Biosystems, Inc.). Cells were counted by trypan blue exclusion with the Countess Automated Cell Counter (Life Technologies, Inc.). The high MOI ensured that essentially 100% of the cells in each culture were transduced and it was assumed that each individual cell in the culture contributed approximately equal amounts of luciferase activity. Reporter expression was then calculated as the relative luciferase activity of each culture divided by the number of cells in that particular culture. Relative reporter expression was then normalized to controls.

2.7. Detection of Cell Surface Markers by Flow Cytometry

Approximately 2×10^{6} cells were harvested and washed with ice-cold Buffer A (phosphate-buffered saline (PBS) with 2 mM EDTA and 5 mg/mL BSA) and resuspended in 100 μL Buffer A plus 10% Human *FcR* Blocking Reagent (Miltenyi Biotec, Bergisch Gladbach, Germany). The following antibodies (BioLegend, Inc., San Diego, CA) were used: APC conjugated mouse-anti human CD11b, APC-Cy7 conjugated mouse-anti human CD14. Cells were washed and resuspended in 200 μL Buffer A, with 10 μM DAPI added just prior to flow cytometric analysis on a BD Biosciences LSR-II bench-top flow cytometer, located in the University of Kansas Medical Center Flow Cytometry Core Laboratory. Non-transduced, high viability cells were used to determine gate positions for viability (DAPI) and GFP positivity.

2.8 Gene Expression Analyses

2.8.1. Gene Expression Profiling by Microarray Analysis—Gene profiling was carried out at the Kansas University School of Medicine Microarray Facility. Total RNA was purified from test samples (U937 ± Dox, ± PMA) using the RNeasy MicroKit (Qiagen, Inc.). The concentration and purity of total RNA was assessed with an Agilent Bioanalyzer. Biotinylated cRNA was synthesized from the RNA and hybridized to high density Affymetrix human GeneChips HG-U133 Plus 2.0 (Affymetrix, Inc., Santa Clara, CA). Preliminary data analysis was performed using the AltAnalyze software suite to perform statistical analyses and generate log2 fold expression values normalized to on-plate controls (Emig et al., 2010). Log2 values were imported and analysed with Mayday to generate relative expression heatmaps (Battke et al., 2010). Gene ontology (GO) term association analysis was performed by obtaining a probeset displaying greater than 2-fold activation upon PMA treatment and a degree of impairment less than −1.3 (where impairment is the fold expression difference between the PMA treated sample and the PMA+Dox treated sample, a negative value indicates reduced expression; a total of 182 probes were obtained using these filters) and submitting the probelist to the Database for Annotation, Visualization and Integrated Discovery (DAVID) web-based server (Huang da et al., 2009a; Huang da et al., 2009b; Huang da et al., 2009c). Data were deposited in the NCBI GEO database (accession GSE45417).

2.8.2. Quantitative Real Time Reverse Transcriptase PCR (qRT-PCR)—Total RNA was isolated using TRIZOL reagent (Sigma-Aldrich, Inc.) according to the manufacturer's instruction and quantitated. For cDNA synthesis, 0.5 μg total RNA was reverse transcribed with the Verso cDNA kit RT-PCR system according to the manufacturer's protocol (Thermo Scientific, Inc.). 1 μL of the reverse transcription reaction was combined with appropriate primers (Supplemental Table I) and qPCR reaction mix (Maxima SYBR Green/Fluorescein qPCR reagent, Thermo Scientific, Inc.). The reactions were carried out in an iCycler real-time thermal cycler equipped with a MyiQ single color real time PCR detection system (Bio-Rad Laboratories, Inc.). Each primer pair was optimized to verify specificity, by melting curve analysis and to ensure efficiency was >95%. Accordingly, data were then analyzed by the $2^{-\Delta\Delta Ct}$ method as described (Livak and Schmittgen, 2001).

2.9. Chromatin immunoprecipitation

Purification of chromatin and chromatin immunoprecipitation was performed essentially as described (Carey et al., 2009). Sonication of 2×10^7 U937 cells per ml of nuclear lysis buffer (Carey et al., 2009) was conducted with a Microson XL Sonicator (Misonix, Inc.) 20 × 20 second bursts, setting 5. For all ChIP reactions, 5 μg of antibody was used. Protein-A/G magnetic beads (New England Biolabs, Inc.) were used to collect immune-complexes. DNA was purified from eluted chromatin with the Gel/PCR DNA Fragment Purification Kit (IBI Scientific, Inc.). For ChIP the following antibodies were used: anti-ZXDC directed against the N-terminus (Al-Kandari et al., 2007a), mouse anti-human BCL6 (IG191E/A8; BioLegend, Inc.) and control normal rabbit IgG (Cell Signaling, Inc.). Co-immunoprecipitated DNA was quantified by real time PCR. Primers used in the real time PCR reactions are listed Supplemental Table I.

2.10. Transfection, co-immunoprecipitation and Western blotting

Co-IPs and Western blot were performed as previously described (Al-Kandari et al., 2007b). Co-IPs of endogenous ZXDC1 and BCL6 proteins were performed with Raji cell extracts whereas all co-immunoprecipitations involving exogenously expressed proteins were carried out in HEK293 cells transfected with 2 μg total plasmid using Turbofect Reagent (Fermentas, Inc.) according to manufacturer's instructions. Antibodies against FLAG tag (M2; Sigma-Aldrich, Inc.) and HA tag (clone 12CA5; Roche Applied Science, Inc., Indianapolis, IN) were used for IP and Western blot. Detection was carried out using the ECL-Plus Reagent (GE Healthcare, Inc., Piscataway, NJ) and visualized using a Typhoon Variable Mode Imager (GE Healthcare, Inc.).

2.11. Confocal Microscopy

Approximately 4×10^4 U937 were washed with phosphate buffered saline and affixed to glass microscope slides via cytospin centrifugation at 400 rpm for 3 minutes (Shandon Cytospin 3, Thermo Scientific, Inc.). Cells were fixed with 2% paraformaldehyde in PBS for 15 minutes at room temperature, permeabilized with 1% Triton X-100 in PBS for 15 minutes and blocked with PBS + 10% normal goat serum for 1 hour at 37°C. Slides were incubated with primary antibody solutions (5 μg/mL in PBS + 1% normal goat serum) for 16h at 4°C, followed by incubation with secondary antibody solutions (1 μg/mL in PBS + 1% normal goat serum). For co-localization studies the following antibodies were used: anti-ZXDC directed against the N-terminus (Al-Kandari et al., 2007a), mouse anti-human BCL6 (IG191E/A8; BioLegend, Inc.), goat anti-mouse IgG-FITC (Life Technologies, Inc.) and goat-anti rabbit IgG-Cy5 (GeneTex, Inc., San Antonio, Tx). Slides were mounted with SlowFade Gold anti-fade reagent with DAPI mounting media (Life Technologies, Inc.) and

cover-slipped. Samples were analyzed on a Leica TCS SPE confocal fluorescent microscope (University of Kansas Confocal Imaging Facility).

3. Results

3.1. Expression of ZXDC protein declines following differentiation of U937 cells with PMA

We originally identified the *ZXDC* cDNA by yeast two-hybrid with the class II trans-activator (CIITA) as bait (Al-Kandari et al., 2007a) and subsequently demonstrated that ZXDC forms a heterodimer with co-family member ZXDA, which is necessary for robust transcription of MHC class II genes (Al-Kandari et al., 2007b). *ZXDC* is ubiquitously expressed, though it has relatively higher expression in cells of the hematopoietic lineage. Analysis of published gene expression profiles indicates ZXDC expression is enriched in cells of the myeloid lineage and in particular, is highly expressed in granulocytes (Benita et al., 2010; Payton et al., 2009). Expression is relatively lower in cells of monocytic lineage and in cells at earlier stages of differentiation.

To assess expression of ZXDC in a model of monocyte differentiation, we treated U937 cells with phorbol 12-myristate 13-acetate (PMA) and measured ZXDC protein levels by Western blot. Using an antibody raised against the N-terminus of the two major ZXDC isoforms (Al-Kandari et al., 2007a) we observed two immunoreactive species that are differentially expressed during a 72h PMA treatment time course (Figure 1A). The observed ZXDC2 isoform with an apparent molecular mass (M_{app}) of approximately 95 kDa (predicted M = 74.8 kDa) arises through transcriptional termination within the seventh intron in contrast to ZXDC1 (M_{app} ~130 kDa, predicted M = 91 kDa) which terminates in exon eleven (Figure 1B). The sumoylated form of ZXDC1 (upper band) was also detected (Jambunathan and Fontes, 2007). Differentiation of U937 resulted in reduced expression of ZXDC1 protein levels with no significant change in ZXDC2 levels, as assessed by western blot and subsequent densitometry analysis (Fig. 1C), results that were mirrored at the mRNA level, as determined by qRT-PCR (Figure 1D).

3.2. Forced expression of ZXDC1 enhances differentiation of U937

To test if ZXDC isoforms influence U937 differentiation, we forced expression of ZXDC isoforms in U937 cells by lentiviral transduction (Supplemental Figure 1A). We then measured markers of differentiation by flow cytometry of transduced (GFP positive) cells. Overexpression of ZXDC1 resulted in a significant increase in surface expression of *CD11b* (a common myeloid marker) and *CD14* (a marker of monocyte/macrophage differentiation) when compared to cells transduced with a control lentiviral construct (Figure 2A,D). ZXDC2 overexpression showed only a slight effect on CD11b surface expression in the un-induced state (Figure 2B,D.

Treatment of cells with PMA for 72h caused an increase in surface expression of *CD11b* and *CD14,* which was augmented by overexpression of ZXDC1 (Figure 2A,D), but not ZXDC2 (Figure 2B,C). This result is consistent with the notion that ZXDC1 aids in the process of macrophage differentiation. The decline in ZXDC1 expression we observed (Figure 1) perhaps represents aberrant regulation of the gene in U937 which may contribute to the cells' inability to fully differentiate (Harris and Ralph, 1985). Interestingly, additional phenotypic changes typical of macrophage differentiation were not readily detectable in ZXDC1 and ZXDC2 overexpressing cells compared to controls. For example, Giemsa-Wright stained cytospin preparations of ZXDC1 and ZXDC2 overexpressing cells were morphologically indistinguishable from parallel control cell preparations, as was phagocytic NADPH-oxidase (nitro blue-tetrazolium reduction) activity (data not shown).

To assess the effects of ZXDC isoform knockdown on differentiation, we generated lentiviral vectors that express shRNA targeted to both ZXDC isoforms and performed short-term lentiviral transduction of U937. Through this method, we obtained greater than 50% reduction of both isoforms, as assessed by qRT-PCR and Western blot (Supplemental Figure 1B,C). Reduced ZXDC1/2 expression resulted in a negligible change in un-induced expression of *CD11b* and *CD14, however a significant decrease of marker expression was observed upon PMA-induced differentiation* (Figure, E). A cell line with inducible knockdown of ZXDC1 and ZXDC2 with a shRNAmir targeted to a different location showed similar, albeit more modest results (Supplemental Figure 2A). Additionally, knockdown of ZXDC1/2 in HL60, an alternative model of monocytic differentiation, also resulted in restricted marker expression in response to a differentiating agent (Supplementary Figure 2B). Together, these results show that down-regulation of ZXDC1 and ZXDC2 is not necessary for the PMA-induced differentiation program to proceed, as might be presumed based on the results presented in Figure 1B. Instead, forced ZXDC1 expression actually augmented marker expression in un-induced and induced cells, while knockdown of both isoforms restricted marker expression.

3.3. ZXDC1 regulates expression of genes within the chemokine (C-C motif) locus in U937 cells

In order to identify gene targets of ZXDC during the course of U937 differentiation we analyzed the global gene expression profile of U937 undergoing PMA-induced differentiation, with and without knockdown of ZXDC expression. Total cellular RNA was harvested from U937 stably harboring inducible shRNA targeting ZXDC1/2, that were treated with either vehicle alone (control), PMA alone, doxycycline alone (to induce the shRNA) or PMA and doxycycline. We performed gene expression profiling by microarray on these RNAs.

We sought to identify genes that were activated by PMA, but displayed reduced activation upon ZXDC1/2 knockdown. To do this, we first trimmed the global dataset to include only probes that exhibited statistically significant changes in expression upon PMA treatment (Figure 3A). Of these 19,793 probes, 9,689 displayed significant up-regulation. To identify genes whose expression is governed by ZXDC during PMA-induced activation, we then plotted Log2-transformed relative expression data for PMA treated cells versus that of PMA plus ZXDC knockdown cells (Figure 3B). Those probes that significantly deviated from unity in this plot were considered to be likely candidates for regulation by ZXDC. However, to identify genes activated by ZXDC, we then included only probes that displayed impaired expression upon ZXDC1 knockdown, or negative deviation from unity in this plot. To narrow our list of candidate genes activated by ZXDC, we selected only those probes exhibiting impaired expression greater than three times the root mean square deviation ($3\times RMSD < -0.452$) of all 9,689 probes included in the analysis, greater than 4-fold activation by PMA and assignments to annotated genes. These criteria narrowed the list of candidate probes to 41 (Figure 3C) representing 33 genes. The redundancy of probe coverage from several genes suggests that they may be *bona fide* targets of ZXDC1.

Gene ontology (GO) analysis of ZXDC-sensitive, PMA-inducible genes was performed to identify cellular pathways in which ZXDC might be involved (Table 1). There was significant enrichment for genes associated with monocyte functional maturation (“immune/inflammatory response”, “locomotory behavior” and “chemotaxis/taxis). Within the GO “chemotaxis/taxis” gene grouping were several genes within the chemokine (C-C motif) ligand (CCL) gene locus on chromosome 17 (Figure 3C). We decided to determine if ZXDC1 directly regulates one of the target genes within this locus, *Ccl2*.

3.4. Manipulation of ZXDC1 expression influences CCL2 gene expression

Overexpression of ZXDC1 in U937 cells by lentiviral transduction resulted in a significant upregulation of CCL2 mRNA, 15 fold greater than cells transduced with control lentivirus expressing *Cypridina* luciferase (Figure 4A). Addition of PMA showed a significant synergistic effect (approximately 6 fold over PMA-treated control; Figure 4A). Overexpression of ZXDC2 resulted in no significant increases in CCL2 expression, regardless of treatment (Figure 4A). As expected, the effect of stable knockdown of ZXDC was opposite: knockdown of ZXDC restricted baseline expression of CCL2 only modestly, however it significantly restricted PMA induction (Figure 4B). Taken together, these results confirm what was detected by microarray, that ZXDC1 regulates CCL2 expression.

3.5. Over-expression of ZXDC1 activates a reporter construct containing a BCL6-responsive distal regulatory region of the Ccl2 promoter

In order to identify a region of the *Ccl2* promoter responsive to ZXDC1, we generated reporter constructs derived from a well-characterized portion of the *Ccl2* promoter (Figure 5A). Preliminary attempts to perform transient co-transfection in several human cell lines (U937, HEK-293, HeLa and A549) showed either very low promoter activity or no responsiveness to ZXDC1 overexpression (data not presented). We found, however, that a U937-derived cell line harboring stably integrated reporter construct containing the Ccl2 promoter from −3158 to +73 (relative to the transcriptional start site) was activated by over-expression of ZXDC1 (Figure 5A,B). We generated serial deletions of the Ccl2 promoter (Figure 5A) and mapped the ZXDC-responsive region to −3158/−2154, a sequence that contains the previously described “distal response region” (DRR) (Ping et al., 1999; Ping et al., 1996). We were unable to demonstrate binding of ZXDC1 anywhere within 10 kb of the transcriptional start site by chromatin immunoprecipitation (data not shown). While this may simply be due to technical issues, it raised the possibility that ZXDC1 may regulate *Ccl2* expression through a mechanism other than direct binding to the gene’s promoter DNA. Furthermore, we noted that the full −3158/+73 promoter was not responsive to PMA treatment (data not shown). Previous reports have shown that full activation of Ccl2 by AP-1 proteins activated by interleukin-1 induction is dependent upon TRE sequences located in the far 3′ region of the human Ccl2 gene (Wolter et al., 2008). Our result suggests that synergistic activation of the endogenous Ccl2 gene obtained by ZXDC1 overexpression and AP-1 activation (Figure 4A) requires these far 3′ sequence elements.

It has been reported that BCL6 represses *Ccl2* in human (Seto et al., 2011) and mouse cells (Barish et al., 2010; Toney et al., 2000). We hypothesized that at least part of the mechanism by which ZXDC1 regulates *Ccl2* may be through interference with this repressive mechanism. We first verified that BCL6 repressed our *Ccl2* promoter-reporter U937 cell lines by over-expressing BCL6 via lentiviral transduction. Over-expression of BCL6 in the U937 cell line containing the *Ccl2* promoter (−3158/+73) reporter resulted in reduced expression from the integrated reporter (Figure 5C). Repression of the *Ccl2* reporter by BCL6 required the same region (−3158/−2154) as was necessary for activation by ZXDC1 (Figure 5C). Co-transduction of increasing amounts of ZXDC1 with BCL6 reversed repression of the *Ccl2* reporter by BCL6 in a dose-dependent manner (Figure 5D). Together, these results support a model where ZXDC1 reverses or prevents transcriptional repression of *Ccl2* by BCL6.

The antagonism observed between ZXDC1 and BCL6 with regard to Ccl2 reporter expression raises the question of whether ZXDC1 and/or PMA treatment influences BCL6 levels in U937 cells. Analysis of BCL6 transcript levels by gene expression microarray shows that BCL6 does not respond to inducible ZXDC1/2 knockdown, but is up regulated in response to 72h PMA treatment (refer to NCBI GEO accession GSE45417). We verified

these results by qRT-PCR and found that BCL6 gene expression increases over a 72 hour timeframe in response to PMA treatment (Supplementary Figure 3A), and that stable knockdown of ZXDC1/2 had no significant effect of BCL6 transcript levels after 72 hours of PMA treatment (Supplementary figure 3B). Surprisingly, as determined by western blot, BCL6 protein levels remain relatively constant throughout the PMA treatment (Supplementary Figure 3C,D). These results suggest that antagonism between ZXDC1 and BCL6 occurs at the level of protein-protein interaction.

3.6. ZXDC1 and BCL6 proteins interact via the zinc finger domain of BCL6

Based on our observation that BCL6-mediated repression of a *Ccl2* reporter could be reversed by co-expression of ZXDC1, we hypothesized that the two proteins may directly interact. To test this possibility we performed co-immunoprecipitation using lysates from Raji Burkitt's lymphoma cell line. Immunoprecipitation (IP) of ZXDC1 with N-terminus-targeted anti-ZXDC resulted in co-purification of BCL6, as detected by Western blot with anti-BCL6 antibody (Figure 6A). BLC6 was not detected in preparations immunoprecipitated with IgG (Figure 6A).

BCL6 possesses *POZ* (Poxvirus zinc finger) and *PEST* (enriched in proline (P), glutamic acid (E), serine (S) and threonine(T)) domains that are responsible for transcriptional repression (Bereshchenko et al., 2002; Chang et al., 1996). DNA binding (Mascle et al., 2003) and histone deacetylase (HDAC) recruitment occurs via the zinc finger (ZF) domain of BCL6 (Lemercier et al., 2002). To identify the domains of BCL6 involved in ZXDC1 interactions, we performed co-transfection of 3XFLAG-ZXDC1 with hemagglutinin (HA)-tagged BCL6 domain constructs (Figure 6B) in HEK293 cells, followed by immunoprecipitation and Western blot. As can be seen in Figure 6C, only the deletion of the zinc finger domain of BCL6 (HA-BCL6ΔZF) resulted in a significant reduction of BCL6 binding to ZXDC1. ZXDC1 also bound a peptide containing only the zinc fingers of BCL6 (HA-BCL6-ZF only; Figure 6C). The binding of ZXDC1 to this region suggests that ZXDC1 may interfere with DNA binding (Mascle et al., 2003) and/or HDAC recruitment (Lemercier et al., 2002) by BCL6.

3.7. Loss of ZXDC function promotes increased BCL6 occupancy of the Ccl2 promoter

After activation, BCL6 reestablishes repression of *Ccl2* gene expression by binding to specific promoter sequences and recruiting HDACs to restore repressive histone signatures (Barish et al., 2010; Seto et al., 2011); we hypothesized that ZXDC1 may evict BCL6 from these elements resulting thereby enabling increased expression of CCL2. Chromatin immunoprecipitation of BCL6 coupled with massively parallel sequencing (ChIP-Seq) using mouse bone marrow derived macrophages revealed that BCL6 interacts with a distal element (−12.7 kbp) to achieve repression (Barish et al., 2010). In our model system, we mapped repression of CCL2 by BCL6 to −3158/−2154 of the *Ccl2* promoter. Inspection of the nucleotide sequences in that region revealed a potential BCL6 binding site, matching the consensus 5′-CTTCCT(A/G)GAA-3′ (Figure 7A). We performed ChIP with anti-BCL6 and detected weak occupancy of this site ("−3kb enhancer") in the uninduced state but not a sequence ~3kb upstream ("control region"; Figure 7B). Surprisingly, knockdown of ZXDC1/2 by lentiviral shRNA transduction led to negligible changes in occupancy of the −3kbp enhancer (Figure 7B). Importantly, BCL6 occupancy was much higher following PMA induction in the presence of ZXDC1/2 knockdown than in cell expressing a control shRNA (Figure 7B). This result agrees with our observation that knockdown of ZXDC1/2 reduced PMA induction of CCL2 by approximately 60% (Figure 4B).

In order to address the apparent lack of BCL6 occupancy observed at the −3kb enhancer both before and after 72h of PMA activation, we examined BCL6 occupancy of this element

over a 72 hour time course and how occupancy corresponded to *Ccl2* expression. Similar to what was observed in Figure 7B, we found that in the un-induced state, BCL6 does not constitutively occupy the enhancer at high levels (Figure 7C). Upon PMA stimulation, however, BCL6 interaction with the enhancer increases in a manner parallel to transcriptional activation of the *Ccl2* gene (Figure 7C, D), peaking at 24 hours post induction. Expression of *Ccl2* and BCL6 occupancy similarly decline at 48 and 72 hours post induction. The results of this analysis support a model by which BCL6 maintains the repressed state prior to PMA stimulation by maintaining repressive histone signatures through low-level interactions with the enhancer, and restores the repressed state after PMA stimulation by reestablishing repressive histone signatures through high-level interactions with the enhancer. Based on previous reports, repression likely relies upon subsequent recruitment of co-repressors and HDACs (Barish et al., 2010; Barish et al., 2012; Dhordain et al., 1997; Huynh and Bardwell, 1998; Huynh et al., 2000; Lemercier et al., 2002). Further, this result provides an explanation for why we observed only modest differences in BCL6 occupancy at the −3kb enhancer both prior to, and 72 hours after PMA induction in cells stably expressing control shRNA (Figure 7B). Collectively, the results of the BCL6 ChIP in response to ZXDC1/2 knockdown (Figure 7B), the BCL6 ChIP PMA time course (Figure 7C), and the *Ccl2* gene expression time course suggest that BCL6 represses *Ccl2* gene expression, at least in part, by transiently occupying the *Ccl2* promoter at the −3kb enhancer, and that ZXDC1 negatively influences binding of BCL6 to this region.

3.8. ZXDC1/2 and BCL6 co-localization in the nuclei of U937 increases after PMA induction

Several reports have shown that over-expressed BCL6 localizes to repressive nuclear bodies (Barros et al., 2009; Dhordain et al., 1995; Duan et al., 2012; Hirata et al., 2009; Kinugasa et al., 2007; Lemercier et al., 2002; Mascle et al., 2003) that are believed to be involved in establishing repressive domains associated with newly synthesized DNA during the process of DNA replication (Albagli et al., 1999; Puvion-Dutilleul et al., 2003). Furthermore, during the course of gene de-repression associated with initiation of pro-inflammatory cell signaling events, BCL6 has been shown to dissociate from chromatin (Barros et al., 2009) and translocate to the cytoplasm where it is degraded by the proteasome (Hirata et al., 2009). Based on our results showing that ZXDC1 reverses BCL6-mediated repression of *Ccl2* gene expression (Figure 6D) and interacts with BCL6 via its ZF domain (Figure 7C) we sought to determine if ZXDC1 co-localizes with BCL6 in U937 and whether PMA induction alters the cellular distribution of either protein.

We performed immunofluorescence confocal microscopy on preparations of U937 treated with PMA for various amounts of time that theoretically corresponded to key *Ccl2* gene regulatory events predicted by enhancer occupancy analysis (Figure 7C). Prior to PMA treatment, both ZXDC1/2 and BCL6 appeared broadly distributed throughout the nucleoplasm and appear to show only minor co-localization (Figure 9, No PMA). Neither protein exhibited punctuate staining patterns (so-called “nuclear bodies”) as has been described for exogenously over-expressed BCL6, raising the possibility that these structures are the result of over-expression, *in situ* cellular fractionation (Duan et al., 2012), or occur in a cell-type dependent manner. After four hours of PMA treatment, both proteins begin to partially co-localize as well as accumulate in the nuclear periphery, giving a halo-like appearance similar to what has been reported for endogenous BCL6 protein in human gastric carcinoma cell lines (Hirata et al., 2009). After 24 hours of PMA treatment, co-localization was still observed, although not a distinctively distributed to the nuclear periphery. Additionally, some apparent deposition of both proteins in the extra-nuclear space was observed (Figure 8, bottom row).

4. Discussion

Very limited information exists regarding the function of the three member zinc finger X-linked duplicated (ZXD) family of transcription factors. We have previously shown that ZXDA and ZXDC are necessary for full activation of MHC class II genes by CIITA (Al-Kandari et al., 2007b) but beyond this role, nothing is known. In this report, we demonstrate that one isoform of ZXDC, ZXDC1, influences expression of genes related to monocyte differentiation and function. Based upon our data, ZXDC1 cannot be considered a lineage-determining transcription factor, though it clearly influences expression of genes specific for the monocyte/macrophage lineage. At least part of the mechanism by which ZXDC1 regulates one target gene, *Ccl2*, is the reversal transcriptional repression by BCL6.

Given our findings that ZXDC1 regulates expression of genes associated with differentiated cells, it was surprising that we observed a modest decrease in ZXDC1 proteins levels when the leukemic U937 cell line was differentiated by PMA treatment. This observation may reflect the fact that U937 differentiation is incomplete when compared to peripheral blood-derived monocytes and macrophages (Harris and Ralph, 1985). It is possible that the absence of ZXDC1 elevation in response to PMA stimulation in U937 cells is a consequence of this defect and may in some way contribute to the observed differentiation block of this leukemic cell line. Given that ZXDC1 is also expressed in other blood cell lineages its primary role may be to modify the activity of lineage-specific factors. Such a model would not necessarily dictate that ZXDC protein levels increase upon differentiation. A report of ZXDC interacting with growth factor independence 1 (Gfi-1) supports this notion (Salipante et al., 2009).

Differentiation of U937 with PMA leads to changes in the expression of thousands of genes, a subset of which was sensitive to ZXDC knockdown. Of the many genes involved in chemotaxis, cell cycle and inflammation whose activation by PMA was diminished with ZXDC knockdown, we chose *CCL2* for further analysis. A striking observation is that a reporter construct containing the *Ccl2* promoter was only responsive to ZXDC1 when integrated into the genome of U937. This indicates that either the high copy number achieved by transient transfection was problematic or that a more regular, physiological chromatin environment was necessary for ZXDC1 to achieve transcriptional activation (Carey et al., 2012). We mapped the ZXDC1-responsive region of the *Ccl2* promoter to a ~1000 bp region (−3158/−2154) that contains a previously defined distal regulatory region (DRR) (Cho et al., 2002; Freter et al., 1995; Ping et al., 1999; Ping et al., 1996). We determined that this identical region of the *Ccl2* promoter was also necessary for repression by BCL6.

Our inability to demonstrate direct binding of ZXDC1 within this region led us to hypothesize that ZXDC1 levels may influence the ability of BCL6 to bind the DRR and repress *Ccl2* expression. Our decision to pursue the BCL6 protein as a target of ZXDC1 was influenced by additional factors: BCL6 was shown to directly repress *Ccl2* in conjunction with NCoR/SMRT (Barish et al., 2012); BCL6 regulates many genes within the *Ccl* locus (Seto et al., 2011); BCL6 has previously been shown to be a target of other factors that indirectly activate *Ccl2* gene expression (Lee et al., 2003). Overexpression of ZXDC1 reversed repression of CCL2 gene transcription by BCL6 in a dose-dependent manner. This finding was consistent with our observation that knockdown of ZXDC lead to increased occupancy of the *Ccl2* promoter by BCL6. Although we do not yet know how ZXDC1 alters BCL6 occupancy of the promoter, the fact that the two proteins interact suggest a range of possibilities. It is currently unknown if BCL6-mediated repression of *Ccl2* involves disruption of the long-range interaction between the PRR and DRR of *Ccl2* that occurs during TNFα induction in mouse NIH-3T3 cells, (Boekhoudt et al., 2003; Teferedegne et

al., 2006) or if ZXDC1 enhances these interactions. However, since it has been shown that this long range interaction is facilitated first by association of NF-κB with the DRR followed by histone acetylation, Sp1 binding to the PRR and then DRR-PRR association, it stands to reason that BCL6 association, that is often mutually exclusive of NF-κB binding (Barish et al., 2010), co-repressor association (Dhordain et al., 1997; Ghisletti et al., 2009; Huynh and Bardwell, 1998; Huynh et al., 2000) and HDAC recruitment (Lemercier et al., 2002) precludes this event.

A mounting body of work has demonstrated that BCL6 repressor activity is regulated by post-translation modifications including MAPK-mediated (Moriyama et al., 1997; Niu et al., 1998) and Rac1/PAK1-mediated (Barros et al., 2009) phosphorylation, in addition to p300-mediated acetylation (Bereshchenko et al., 2002) within the PEST domain. Whereas both of these modifications result in de-repression, acetylation leads to dissociation from HDACs and accumulation of acetylated BCL6, while phosphorylation generally results in subsequent ubiquitylation and proteasomal degradation of BCL6 (Duan et al., 2012). It is possible that ZXDC1 influences either the phosphorylation or acetylation status of BCL6, or perhaps the association of ZXDC1 with BCL6 is dependent upon the presence of these modifications. Still, ZXDC1 levels did not influence BCL6 protein levels (data not shown), despite increasing BCL6 mRNA levels slightly (as gauged by microarray), suggesting ZXDC is likely not involved in mediating BCL6 degradation.

An additional level of BCL6 regulation involves interaction with the C-terminal fragment of heparin binding-epidermal growth factor-like growth factor (HB-EGF-CTF). Upon PMA treatment of gastric and fibrosarcoma cancer cell lines HB-EGF-CTF translocates to the nucleus and associates with BCL6, reverses BCL6-mediated repression and facilitates nuclear export of BCL6 to the cytosol where it is eventually degraded (Hirata et al., 2009; Kinugasa et al., 2007). The interaction of HB-EGF-CTF has also been localized to the ZF domain of BCL6 (Kinugasa et al., 2007). We observed the co-localization of ZXDC1 and BCL6 upon PMA stimulation of U937 by immunoflourescent confocal microscopy (Figure 9) where both proteins accumulated in the nuclear periphery, a region sometimes associated, though not absolutely, with transcriptional repression (Deniaud and Bickmore, 2009). Still, we did not observe significant nuclear export of either protein, even after a full 24 hours of PMA exposure. This difference in translocation and subsequent degradation may reflect the critical role BCL6 plays in resolving the inflammatory response in innate immune cell types (Barish et al., 2010) and a cell type-specific aspect of BCL6 regulation.

In this report we have demonstrated that ZXDC1 is a novel transcriptional regulator of key inflammatory genes. While further investigation is warranted to characterize the mechanism of ZXDC1 *in vivo*, our results suggest that since ZXDC1 facilitates activation of numerous pro-inflammatory cytokines that are heavily implicated in chronic inflammatory diseases, ZXDC1 may be a suitable target for clinical intervention of these conditions

Supplementary Material

Refer to Web version on PubMed Central for supplementary material.

Acknowledgments

We would like to thank Dr. Ricardo Dalla-Favera for generously providing the BCL6 deletion constructs, Dr. Joyce Slusser for assistance with flow cytometry and Patricia St. John for assistance with confocal microscopy. We thank the Kansas University Medical Center-Microarray Facility (KUMC-MF) for generating array data sets. The Microarray Facility is supported by the Kansas University-School of Medicine, KUMC Biotechnology Support Facility, the Smith Intellectual and Developmental Disabilities Research Center (HD02528) and the Kansas IDeA Network of Biomedical Research Excellence (RR016475). This research was supported by a grant from the NIAID (AI092516) to J.D.F.

References

Al-Kandari W, Jambunathan S, Navalgund V, Koneni R, Freer M, Parimi N, Mudhasani R, Fontes JD. ZXDC, a novel zinc finger protein that binds CIITA and activates MHC gene transcription. Molecular immunology. 2007a; 44:311–321. [PubMed: 16600381]

Al-Kandari W, Koneni R, Navalgund V, Aleksandrova A, Jambunathan S, Fontes JD. The zinc finger proteins ZXDA and ZXDC form a complex that binds CIITA and regulates MHC II gene transcription. Journal of molecular biology. 2007b; 369:1175–1187. [PubMed: 17493635]

Albagli O, Lantoine D, Quief S, Quignon F, Englert C, Kerckaert JP, Montarras D, Pinset C, Lindon C. Overexpressed BCL6 (LAZ3) oncoprotein triggers apoptosis, delays S phase progression and associates with replication foci. Oncogene. 1999; 18:5063–5075. [PubMed: 10490843]

Aleksandrova A, Galkin O, Koneni R, Fontes JD. An N- and C-terminal truncated isoform of zinc finger X-linked duplicated C protein represses MHC class II transcription. Mol Cell Biochem. 2009; 337:1–7. [PubMed: 19777325]

Barish GD, Yu RT, Karunasiri M, Ocampo CB, Dixon J, Benner C, Dent AL, Tangirala RK, Evans RM. Bcl-6 and NF-kappaB cistromes mediate opposing regulation of the innate immune response. Genes & development. 2010; 24:2760–2765. [PubMed: 21106671]

Barish GD, Yu RT, Karunasiri MS, Becerra D, Kim J, Tseng TW, Tai LJ, Leblanc M, Diehl C, Cerchietti L, Miller YI, Witztum JL, Melnick AM, Dent AL, Tangirala RK, Evans RM. The Bcl6-SMRT/NCoR cistrome represses inflammation to attenuate atherosclerosis. Cell metabolism. 2012; 15:554–562. [PubMed: 22465074]

Barros P, Jordan P, Matos P. Rac1 signaling modulates BCL-6-mediated repression of gene transcription. Molecular and cellular biology. 2009; 29:4156–4166. [PubMed: 19487462]

Battke F, Symons S, Nieselt K. Mayday--integrative analytics for expression data. BMC bioinformatics. 2010; 11:121. [PubMed: 20214778]

Benita Y, Cao Z, Giallourakis C, Li C, Gardet A, Xavier RJ. Gene enrichment profiles reveal T-cell development, differentiation, and lineage-specific transcription factors including ZBTB25 as a novel NF-AT repressor. Blood. 2010; 115:5376–5384. [PubMed: 20410506]

Bereshchenko OR, Gu W, Dalla-Favera R. Acetylation inactivates the transcriptional repressor BCL6. Nature genetics. 2002; 32:606–613. [PubMed: 12402037]

Boekhoudt GH, Guo Z, Beresford GW, Boss JM. Communication between NF-kappa B and Sp1 controls histone acetylation within the proximal promoter of the monocyte chemoattractant protein 1 gene. J Immunol. 2003; 170:4139–4147. [PubMed: 12682245]

Carey MF, Peterson CL, Smale ST. Chromatin immunoprecipitation (ChIP). Cold Spring Harb Protoc. 2009; 2009 pdb prot5279.

Carey MF, Peterson CL, Smale ST. Identifying cis-acting DNA elements within a control region. Cold Spring Harbor protocols. 2012; 2012:279–296. [PubMed: 22383646]

Chang CC, Ye BH, Chaganti RS, Dalla-Favera R. BCL-6, a POZ/zinc-finger protein, is a sequence-specific transcriptional repressor. Proceedings of the National Academy of Sciences of the United States of America. 1996; 93:6947–6952. [PubMed: 8692924]

Cho NH, Seong SY, Huh MS, Kim NH, Choi MS, Kim IS. Induction of the gene encoding macrophage chemoattractant protein 1 by Orientia tsutsugamushi in human endothelial cells involves activation of transcription factor activator protein 1. Infection and immunity. 2002; 70:4841–4850. [PubMed: 12183528]

Covic M, Hassa PO, Saccani S, Buerki C, Meier NI, Lombardi C, Imhof R, Bedford MT, Natoli G, Hottiger MO. Arginine methyltransferase CARM1 is a promoter-specific regulator of NF-kappaB-dependent gene expression. The EMBO journal. 2005; 24:85–96. [PubMed: 15616592]

Deniaud E, Bickmore WA. Transcription and the nuclear periphery: edge of darkness? Current opinion in genetics & development. 2009; 19:187–191. [PubMed: 19231154]

Dent AL, Shaffer AL, Yu X, Allman D, Staudt LM. Control of inflammation, cytokine expression, and germinal center formation by BCL-6. Science (New York, NY. 1997; 276:589–592.

Dhordain P, Albagli O, Ansieau S, Koken MH, Deweindt C, Quief S, Lantoine D, Leutz A, Kerckaert JP, Leprince D. The BTB/POZ domain targets the LAZ3/BCL6 oncoprotein to nuclear dots and mediates homomerisation in vivo. Oncogene. 1995; 11:2689–2697. [PubMed: 8545127]

Dhordain P, Albagli O, Lin RJ, Ansieau S, Quief S, Leutz A, Kerckaert JP, Evans RM, Leprince D. Corepressor SMRT binds the BTB/POZ repressing domain of the LAZ3/BCL6 oncoprotein. Proceedings of the National Academy of Sciences of the United States of America. 1997; 94:10762–10767. [PubMed: 9380707]

Duan S, Cermak L, Pagan JK, Rossi M, Martinengo C, di Celle PF, Chapuy B, Shipp M, Chiarle R, Pagano M. FBXO11 targets BCL6 for degradation and is inactivated in diffuse large B-cell lymphomas. Nature. 2012; 481:90–93. [PubMed: 22113614]

Dull T, Zufferey R, Kelly M, Mandel RJ, Nguyen M, Trono D, Naldini L. A third-generation lentivirus vector with a conditional packaging system. Journal of virology. 1998; 72:8463–8471. [PubMed: 9765382]

Ellis BL, Potts PR, Porteus MH. Creating higher titer lentivirus with caffeine. Human gene therapy. 2011; 22:93–100. [PubMed: 20626321]

Emig D, Salomonis N, Baumbach J, Lengauer T, Conklin BR, Albrecht M. AltAnalyze and DomainGraph: analyzing and visualizing exon expression data. Nucleic acids research. 2010; 38:W755–762. [PubMed: 20513647]

Freter RR, Alberta JA, Lam KK, Stiles CD. A new platelet-derived growth factor-regulated genomic element which binds a serine/threonine phosphoprotein mediates induction of the slow immediate-early gene MCP-1. Molecular and cellular biology. 1995; 15:315–325. [PubMed: 7799939]

Ghisletti S, Huang W, Jepsen K, Benner C, Hardiman G, Rosenfeld MG, Glass CK. Cooperative NCoR/SMRT interactions establish a corepressor-based strategy for integration of inflammatory and anti-inflammatory signaling pathways. Genes & development. 2009; 23:681–693. [PubMed: 19299558]

Harris P, Ralph P. Human leukemic models of myelomonocytic development: a review of the HL-60 and U937 cell lines. Journal of leukocyte biology. 1985; 37:407–422. [PubMed: 3855947]

Hirata Y, Ogasawara N, Sasaki M, Mizushima T, Shimura T, Mizoshita T, Mori Y, Kubota E, Wada T, Tanida S, Kataoka H, Kamiya T, Higashiyama S, Joh T. BCL6 degradation caused by the interaction with the C-terminus of pro-HB-EGF induces cyclin D2 expression in gastric cancers. British journal of cancer. 2009; 100:1320–1329. [PubMed: 19337254]

Huang da W, Sherman BT, Lempicki RA. Bioinformatics enrichment tools: paths toward the comprehensive functional analysis of large gene lists. Nucleic acids research. 2009a; 37:1–13. [PubMed: 19033363]

Huang da W, Sherman BT, Lempicki RA. Systematic and integrative analysis of large gene lists using DAVID bioinformatics resources. Nature protocols. 2009b; 4:44–57.

Huang da W, Sherman BT, Zheng X, Yang J, Imamichi T, Stephens R, Lempicki RA. Extracting biological meaning from large gene lists with DAVID. Current protocols in bioinformatics / editoral board, Andreas D. Baxevanis … [et al.]. 2009c; Chapter 13(Unit 13):11.

Huynh KD V, Bardwell J. The BCL-6 POZ domain and other POZ domains interact with the co-repressors N-CoR and SMRT. Oncogene. 1998; 17:2473–2484. [PubMed: 9824158]

Huynh KD, Fischle W, Verdin E, Bardwell VJ. BCoR, a novel corepressor involved in BCL-6 repression. Genes & development. 2000; 14:1810–1823. [PubMed: 10898795]

Jambunathan S, Fontes JD. Sumoylation of the zinc finger protein ZXDC enhances the function of its transcriptional activation domain. Biological chemistry. 2007; 388:965–972. [PubMed: 17696781]

Kinugasa Y, Hieda M, Hori M, Higashiyama S. The carboxyl-terminal fragment of pro-HB-EGF reverses Bcl6-mediated gene repression. The Journal of biological chemistry. 2007; 282:14797–14806. [PubMed: 17392284]

Le Y, Zhou Y, Iribarren P, Wang J. Chemokines and chemokine receptors: their manifold roles in homeostasis and disease. Cellular & molecular immunology. 2004; 1:95–104. [PubMed: 16212895]

Lee CH, Chawla A, Urbiztondo N, Liao D, Boisvert WA, Evans RM, Curtiss LK. Transcriptional repression of atherogenic inflammation: modulation by PPARdelta. Science (New York, NY. 2003; 302:453–457.

Lemercier C, Brocard MP, Puvion-Dutilleul F, Kao HY, Albagli O, Khochbin S. Class II histone deacetylases are directly recruited by BCL6 transcriptional repressor. The Journal of biological chemistry. 2002; 277:22045–22052. [PubMed: 11929873]

Livak KJ, Schmittgen TD. Analysis of relative gene expression data using real-time quantitative PCR and the 2(-Delta Delta C(T)) Method. Methods (San Diego, Calif. 2001; 25:402–408.

Marino MP, Luce MJ, Reiser J. Small- to large-scale production of lentivirus vectors. Methods in molecular biology (Clifton, NJ). 2003; 229:43–55.

Martin T, Cardarelli PM, Parry GC, Felts KA, Cobb RR. Cytokine induction of monocyte chemoattractant protein-1 gene expression in human endothelial cells depends on the cooperative action of NF-kappa B and AP-1. European journal of immunology. 1997; 27:1091–1097. [PubMed: 9174597]

Mascle X, Albagli O, Lemercier C. Point mutations in BCL6 DNA-binding domain reveal distinct roles for the six zinc fingers. Biochemical and biophysical research communications. 2003; 300:391–396. [PubMed: 12504096]

Moriyama M, Yamochi T, Semba K, Akiyama T, Mori S. BCL-6 is phosphorylated at multiple sites in its serine- and proline-clustered region by mitogen-activated protein kinase (MAPK) in vivo. Oncogene. 1997; 14:2465–2474. [PubMed: 9188861]

Naldini L, Blomer U, Gage FH, Trono D, Verma IM. Efficient transfer, integration, and sustained long-term expression of the transgene in adult rat brains injected with a lentiviral vector. Proceedings of the National Academy of Sciences of the United States of America. 1996; 93:11382–11388. [PubMed: 8876144]

Niu H, Ye BH, Dalla-Favera R. Antigen receptor signaling induces MAP kinase-mediated phosphorylation and degradation of the BCL-6 transcription factor. Genes & development. 1998; 12:1953–1961. [PubMed: 9649500]

Payton JE, Grieselhuber NR, Chang LW, Murakami M, Geiss GK, Link DC, Nagarajan R, Watson MA, Ley TJ. High throughput digital quantification of mRNA abundance in primary human acute myeloid leukemia samples. The Journal of clinical investigation. 2009; 119:1714–1726. [PubMed: 19451695]

Ping D, Boekhoudt GH, Rogers EM, Boss JM. Nuclear factor-kappa B p65 mediates the assembly and activation of the TNF-responsive element of the murine monocyte chemoattractant-1 gene. J Immunol. 1999; 162:727–734. [PubMed: 9916692]

Ping D, Jones PL, Boss JM. TNF regulates the in vivo occupancy of both distal and proximal regulatory regions of the MCP-1/JE gene. Immunity. 1996; 4:455–469. [PubMed: 8630731]

Puvion-Dutilleul F, Souquere-Besse S, Albagli-Curiel O. The relationship between BCL6 bodies and nuclear sites of normal and halogenated DNA and RNA synthesis. Microscopy research and technique. 2003; 61:389–407. [PubMed: 12811744]

Rahimi P, Wang CY, Stashenko P, Lee SK, Lorenzo JA, Graves DT. Monocyte chemoattractant protein-1 expression and monocyte recruitment in osseous inflammation in the mouse. Endocrinology. 1995; 136:2752–2759. [PubMed: 7750500]

Rollins BJ, Walz A, Baggiolini M. Recombinant human MCP-1/JE induces chemotaxis, calcium flux, and the respiratory burst in human monocytes. Blood. 1991; 78:1112–1116. [PubMed: 1868242]

Salipante SJ, Rojas ME, Korkmaz B, Duan Z, Wechsler J, Benson KF, Person RE, Grimes HL, Horwitz MS. Contributions to neutropenia from PFAAP5 (N4BP2L2), a novel protein mediating transcriptional repressor cooperation between Gfi1 and neutrophil elastase. Molecular and cellular biology. 2009; 29:4394–4405. [PubMed: 19506020]

Seto T, Yoshitake M, Ogasawara T, Ikari J, Sakamoto A, Hatano M, Hirata H, Fukuda T, Kuriyama T, Tatsumi K, Tokuhisa T, Arima M. Bcl6 in pulmonary epithelium coordinately controls the expression of the CC-type chemokine genes and attenuates allergic airway inflammation. Clin Exp Allergy. 2011; 41:1568–1578. [PubMed: 21801248]

Shyy JY, Lin MC, Han J, Lu Y, Petrime M, Chien S. The cis-acting phorbol ester “12-O-tetradecanoylphorbol 13-acetate”-responsive element is involved in shear stress-induced monocyte chemotactic protein 1 gene expression. Proceedings of the National Academy of Sciences of the United States of America. 1995; 92:8069–8073. [PubMed: 7644539]

Teferedegne B, Green MR, Guo Z, Boss JM. Mechanism of action of a distal NF-kappaB-dependent enhancer. Molecular and cellular biology. 2006; 26:5759–5770. [PubMed: 16847329]

Theofilopoulos AN, Gonzalez-Quintial R, Lawson BR, Koh YT, Stern ME, Kono DH, Beutler B, Baccala R. Sensors of the innate immune system: their link to rheumatic diseases. Nat Rev Rheumatol. 2010; 6:146–156. [PubMed: 20142813]

Toney LM, Cattoretti G, Graf JA, Merghoub T, Pandolfi PP, Dalla-Favera R, Ye BH, Dent AL. BCL-6 regulates chemokine gene transcription in macrophages. Nature immunology. 2000; 1:214–220. [PubMed: 10973278]

Ueda A, Okuda K, Ohno S, Shirai A, Igarashi T, Matsunaga K, Fukushima J, Kawamoto S, Ishigatsubo Y, Okubo T. NF-kappa B and Sp1 regulate transcription of the human monocyte chemoattractant protein-1 gene. J Immunol. 1994; 153:2052–2063. [PubMed: 8051410]

Wolter S, Doerrie A, Weber A, Schneider H, Hoffmann E, von der Ohe J, Bakiri L, Wagner EF, Resch K, Kracht M. c-Jun controls histone modifications, NF-kappaB recruitment, and RNA polymerase II function to activate the ccl2 gene. Molecular and cellular biology. 2008; 28:4407–4423. [PubMed: 18443042]

Ye BH, Cattoretti G, Shen Q, Zhang J, Hawe N, de Waard R, Leung C, Nouri-Shirazi M, Orazi A, Chaganti RS, Rothman P, Stall AM, Pandolfi PP, Dalla-Favera R. The BCL-6 proto-oncogene controls germinal-centre formation and Th2-type inflammation. Nature genetics. 1997; 16:161–170. [PubMed: 9171827]

Highlights

- Transcription factor ZXDC1 promotes differentiation of the leukemia cell line U937.
- ZXDC1 activates macrophage-specific and pro-inflammatory gene clusters
- ZXDC1 reverses inhibition of CCL2 expression via eviction of the repressor BCL6

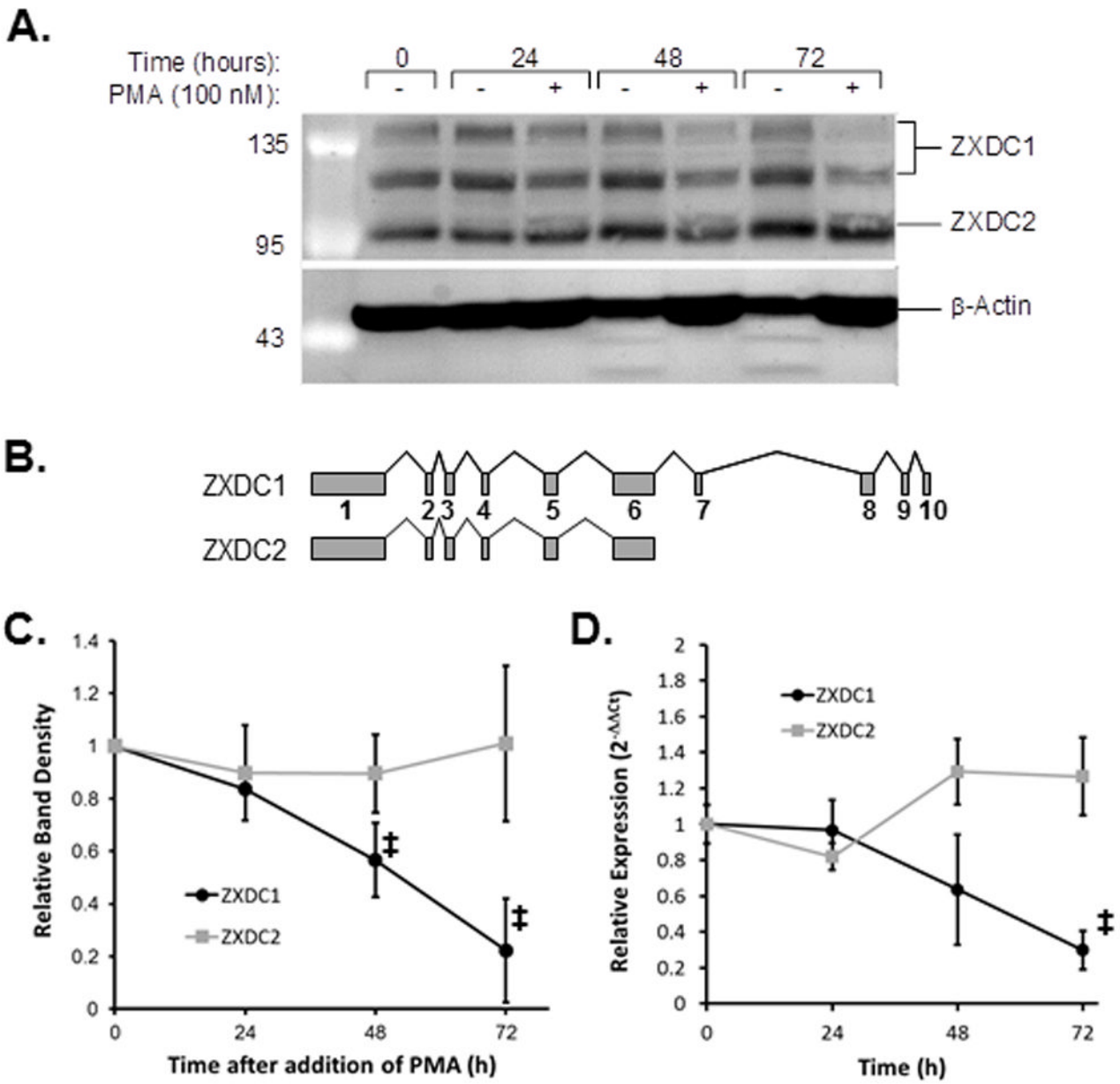

Figure 1. Expression of ZXDC isoforms during PMA-induced differentiation of U937

A, Time course of PMA treatment of U937 shows that ZXDC isoforms are differentially expressed during differentiation as detected by Western blot. The bands labeled ZXDC1 represent the sumoylated (upper) and unmodified (lower) forms. B, Schematic of ZXDC gene and exons included in ZXDC1 and ZXDC2. ZXDC2 is derived from alternative transcriptional termination site usage within the sixth intron. C, Relative band intensities from western blots (as shown in A) for ZXDC1 (black circles) and ZXDC2 (grey bars) were measured by densitometry and normalized to intensities obtained for β-Actin which was used as a loading control. D, Time course of PMA treatment analyzed by qRT-PCR incorporating primers specific for ZXDC1 (black circles) and ZXDC2 (grey squares). Values reported represent the means (± s.d.) of three independent experiments. ‡$P < 0.05$.

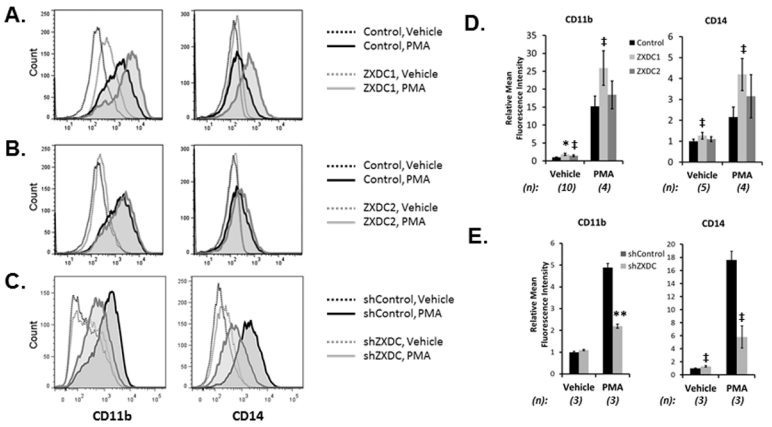

Figure 2. Effect of ZXDC level manipulation on monocyte-specific surface marker expression in U937

U937 cells were transduced with lentiviral vectors expressing (A) ZXDC1, or (B) ZXDC2, or (C) shRNA targeting ZXDC1/2. Cells were treated with vehicle (dashed lines) or PMA (solid lines) for 72h and expression of indicated surface antigens was assessed by flow cytometry. Black traces: transduced with control lentivirus; Gray traces: transduced with expression lentivirus as indicated. Only transduced cells (GFP positive) were included in the analyses. Mean fluorescence intensities obtained for the indicated surface antigens from individual independent experiments were normalized to compare the effects of ZXDC1/2 overexpression (D; Black bars: transduction with control lentivirus; light grey bars: transduction with ZXDC1 overexpressing lentivirus; dark grey bars: transduction with ZXDC2 overexpressing lentivirus), and knockdown of ZXDC1/2 (E; Black bars: transduction with control shRNA lentivirus; grey bars: transduction with ZXDC1/2 specific shRNA lentivirus). Bars represent the means of n (indicated) biological replicates +/− s.d.. **P < 0.005, *P < 0.01, ‡P < 0.05.

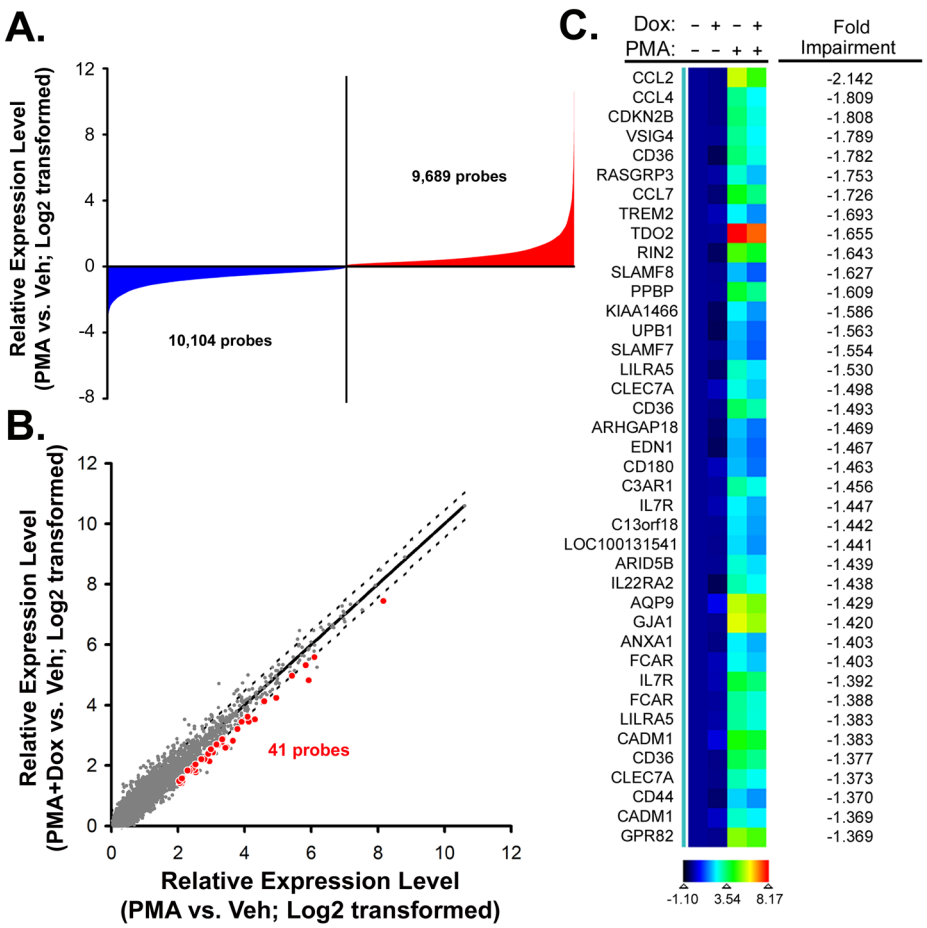

Figure 3. Differential gene expression caused by knockdown of ZXDC in U937 cells treated with PMA for 72 hours as identified by microarray

A, Probes exhibiting significant expression changes upon PMA treatment. B, Detection of probes up-regulated by PMA whose expression is significantly altered by ZXDC knockdown. The solid line represents no change (unity); dashed lines represent ± three times the RMSD of all probes up-regulated by PMA. Probes in red represent those exhibiting > 4-fold PMA activation and significant impairment upon ZXDC knockdown. C, Genes whose activation by PMA was impaired by knockdown of ZXDC in U937 cells. Results are presented as the means of biological triplicates.

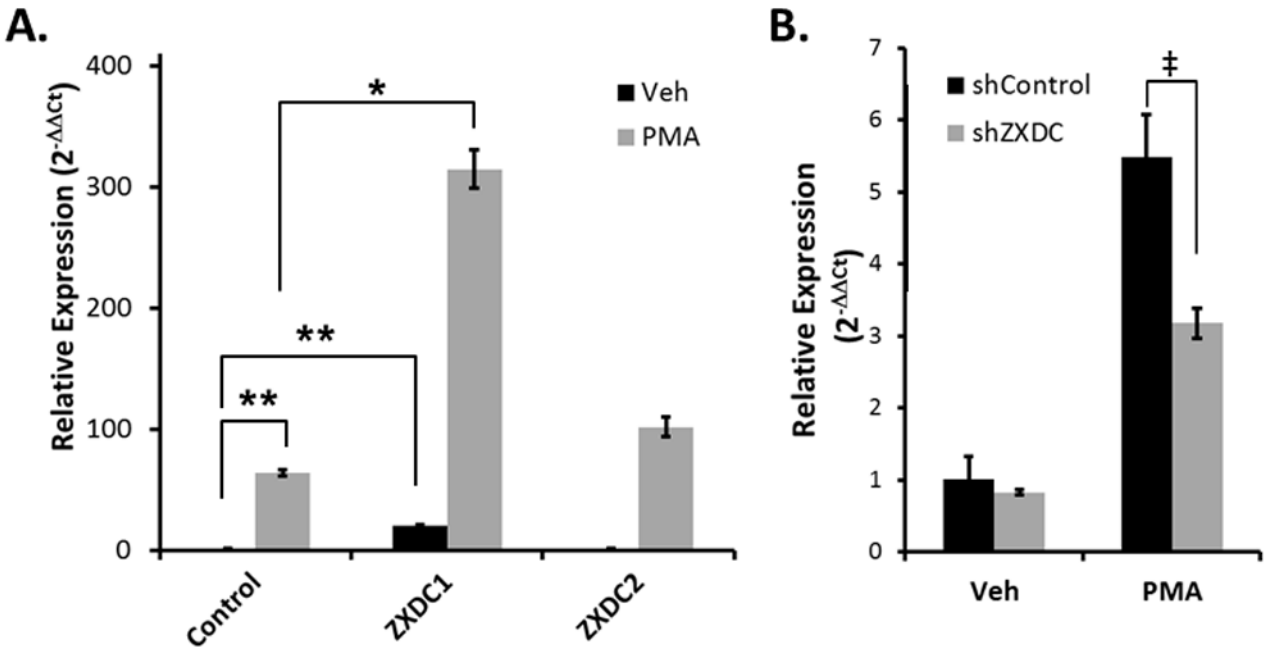

Figure 4. *Ccl2* gene expression was activated by over-expression of ZXDC1 but not ZXDC2

A, U937 were transiently transduced with lentivirus expressing ZXDC1, ZXDC2 or control as indicated 96 hours prior to treatment with vehicle (black bars) or PMA (gray bars) for 72h and analyzed by qRT-PCR to measure *Ccl2* expression. B, U937 were transiently transduced with lentiviral vectors expressing either shRNA against ZXDC1/2 (shZXDC, grey bars) or luciferase (shControl, black bars) for 96 hours prior to treatment with vehicle or PMA for 72h and analyzed by qRT-PCR to measure *Ccl2* expression. Bars represent the means of three biological replicates +/− s.d. **P < 0.005, *P < 0.01, † < 0.02.

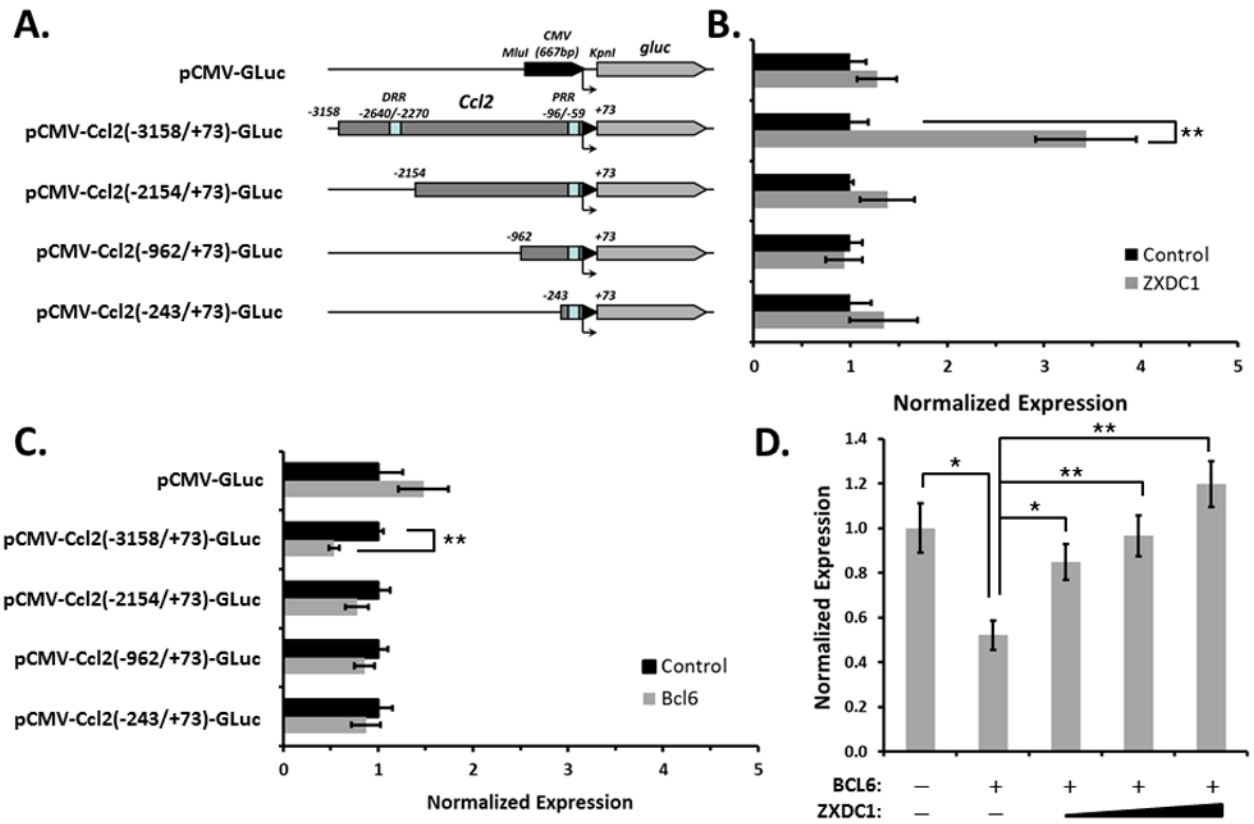

Figure 5. Identification of an overlapping ZXDC1 and BCL6 responsive element in the *Ccl2* gene promoter

A, Schematic of *Ccl2* Gaussia-luciferase reporter constructs used to generate stable U937 reporter cell lines. Coordinates are with respect to the transcriptional start site of *Ccl2*. B, U937 reporter cell lines were transduced with lentivirus expressing ZXDC1 (gray bars) or vector (black bars) followed by luciferase assay 48 hours later. C. U937 reporter cell lines were transduced with lentivirus expressing BCL6 (gray bars) or vector (black bars) and analyzed as in (B). D, U937 reporter cell line stable for the (−3158/+73) reporter construct were transduced with lentivirus expressing BCL6 alone or with increasing amounts of lentivirus expressing ZXDC, as indicated, and analyzed as in (B). Bars represent the means of three biological replicates +/− s.d. **P < 0.005, *P < 0.01.

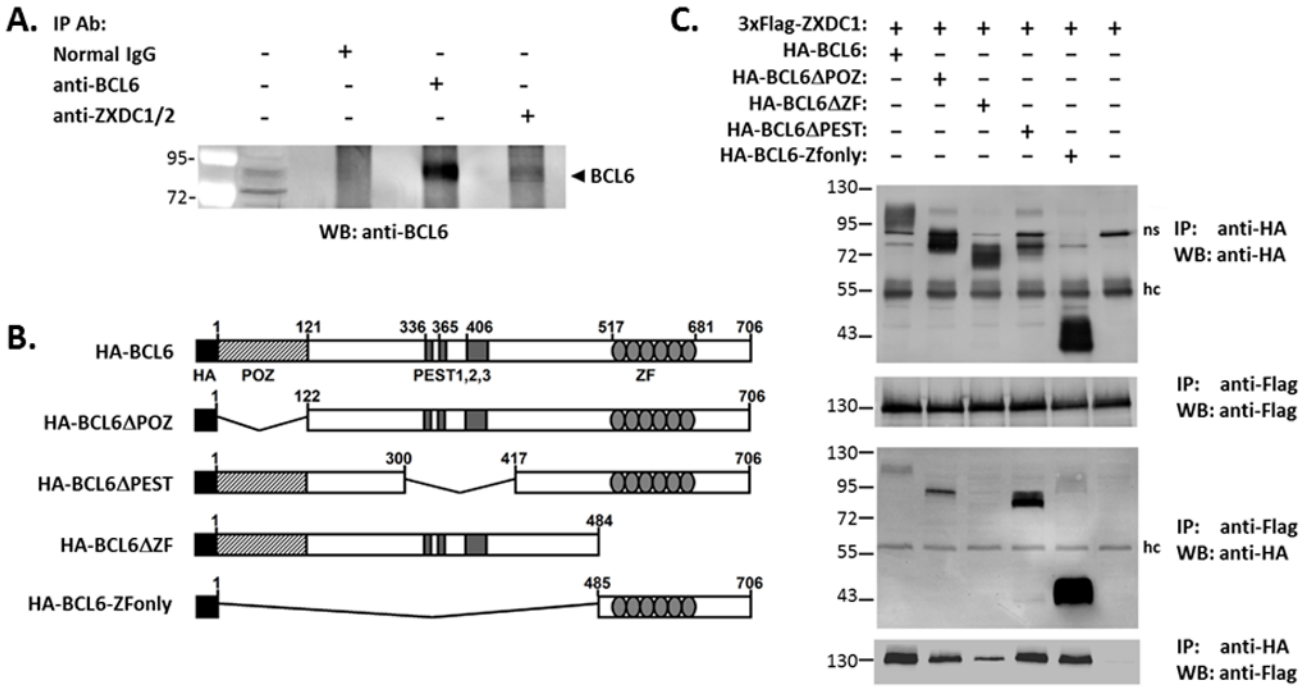

Figure 6. ZXDC1 interacts with BCL6 via its zinc finger (ZF) domain region

A, Raji cell lysates were subjected to immunoprecipitation with the indicated antibodies followed by Western blot with anti-BCL6. The first lane contains cellular lysate. B, Schematic representation of BCL6 and domain deletion derivatives used in transient transfection experiments. C, HEK293 cells were transfected with the indicated expression plasmids, followed by immunoprecipitation with anti-FLAG (ZXDC) or anti-HA (BCL6). Western blot was performed on the immunoprecipitates as indicated; ns: non-specific band, hc: IgG heavy chain.

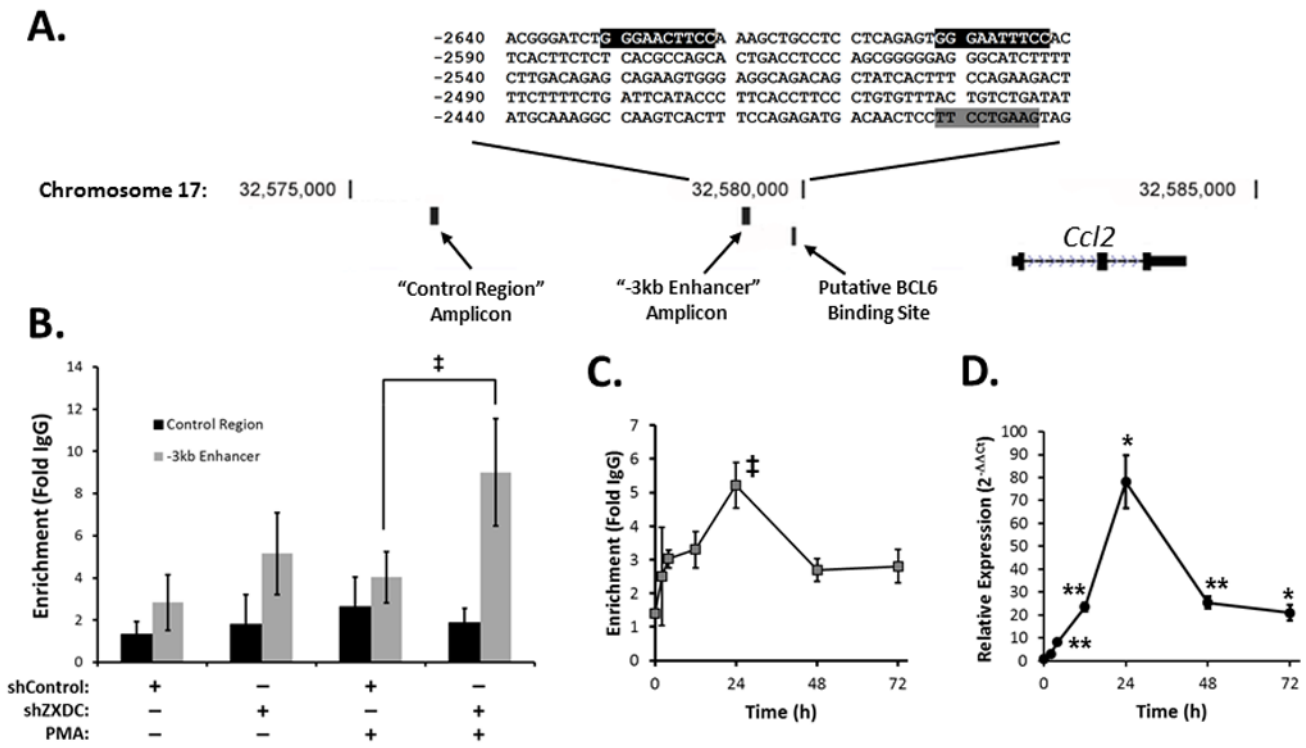

Figure 7. Loss of ZXDC function promotes increased BCL6 occupancy of the *Ccl2* distal regulatory element

A, Inspection of the *Ccl2* promoter distal response region (DRR) sequence revealed the presence of a putative BCL6 binding site (grey highlight) co-localized with an opposing, well established pair of NF-κB binding sites (black higlights) (Ping et al., 1999; Ping et al., 1996). Location of ChIP amplicons are indicated in relation to the putative BCL6 binding site. B, U937 cells stably expressing a shRNA targeting either ZXDC1/2 (shZXDC) or a control shRNA (shControl) were treated with vehicle or PMA for 72 hours. Chromatin was prepared and subjected to immunoprecipitation with anti-BCL6 or control IgG antibody followed by qRT-PCR on the isolated DNA with primers specific for amplification of either the "−3kb Enhancer" (grey bars), or a "Control Region" of genomic DNA, approximately 3.5kb usptream of the putative BLC6 binding site (black bars). Data is represented as "Fold IgG"; the amount of anti-BCL6 immunoprecipitated DNA (normalized to input) divided by the amount of normal IgG immunoprecipitated DNA (also normalized to input). C, Analysis of BCL6 occupancy of the −3kb enhancer throughout a 72 hour PMA treatment time course by ChIP. Data was analyzed as in B. D, Measurement of corresponding *CCL2* gene expression by qRT-PCR from samples used for ChIP analysis in C. Data is represented as the mean of, at minimum,3 biological replicates +/− s.d. **P < 0.005, *P < 0.01, ‡P < 0.05).

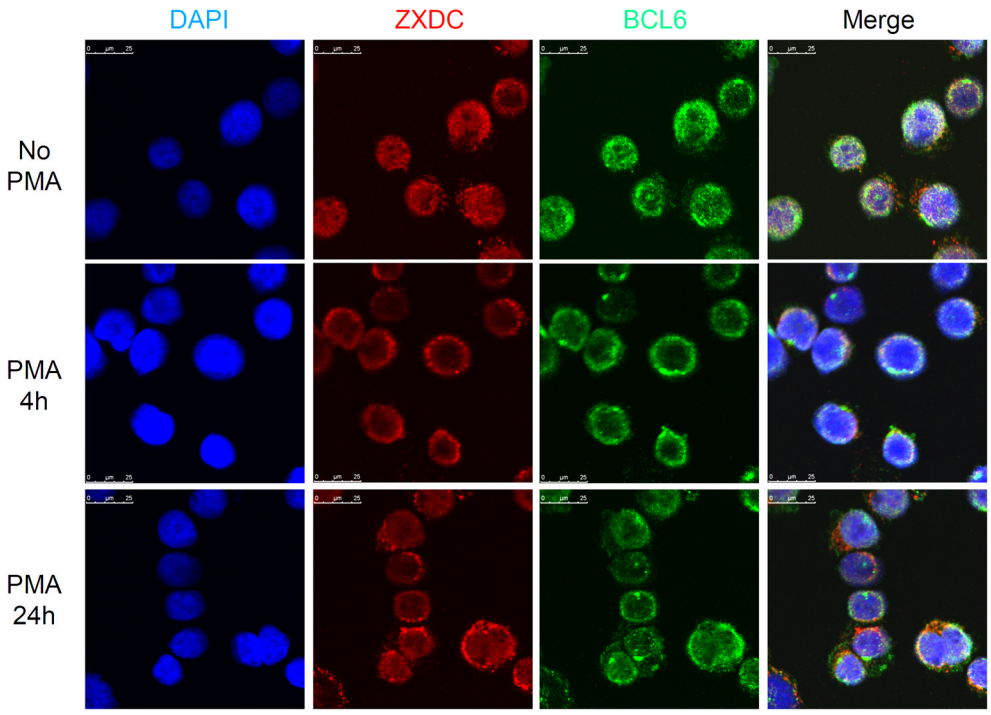

Figure 8. Co-localization of ZXDC1 and BCL6 in the nuclei of U937 increases after PMA induction

U937 were treated with PMA for the indicated times and attached to slides via cytospin. Endogenous ZXDC1/2 and BCL6 proteins were stained with specific antibodies and visualized by confocal fluorescent microscopy.

Table 1

Gene ontology anaysis of PMA-inducible, ZXDC-responsive genes

Gene probes exhibiting differential expression caused by induction of ZXDC-specific shRNA in U937 cells treated with PMA for 72 h identified by AffymetrixU133A 2.0 microarray were subjected to Gene Ontology (GO) term association analysis (Database for Annotation, Visualization and Integrated Discovery (DAVID) web-based server (Huang da et al., 2009a; Huang da et al., 2009b; Huang da et al., 2009c)). Those probes displaying greater than 2-fold activation upon PMA treatment and a degree of impairment less than −1.3 (182 probes) were included in the analysis.

GO Term	Number of genes	P value
Immune response	21	1.2×10^{-7}
Response to wounding	16	7.6×10^{-6}
Inflammatory response	12	2.7×10^{-5}
Locomotory behavior	11	3.4×10^{-5}
Defense response	16	4.3×10^{-5}
Chemotaxis	8	1.8×10^{-4}
Taxis	8	1.8×10^{-4}
Response to organic substance	16	2.5×10^{-4}
Regulation of apoptosis	17	2.6×10^{-4}
Regulation of programmed cell death	17	2.9×10^{-4}